View Planning with a Registration Component

Scott, William; Roth, Gerhard; Rivest, J.-F.

National Research Council Canada
Conseil national de recherches Canada

Institute for Information Technology
Institut de Technologie de l'information

NRC·CNRC

*View Planning with a Registration Component**

W.R. Scott, G. Roth, and J.-F. Rivest
May 2001

***published in** Proceedings of the 3D Imaging and Modeling Conference (3DIM), Quebec, Quebec. May 28–June 1, 2001. NRC 44166.

View Planning with a Registration Constraint

William R. Scott[†‡], Gerhard Roth[‡], Jean-François Rivest[†]

[†] Department of Electrical Engineering,
University of Ottawa, Ottawa, Canada, K1N 6N5
rivest@site.uottawa.ca

[‡] Visual Information Technology Group,
National Research Council of Canada, Ottawa, Canada, K1A 0R6
(william.scott,gerhard.roth)@nrc.ca

Abstract

The view planning problem, also known as the next-best-view (NBV) problem, for object reconstruction and inspection has been shown to be isomorphic to the set covering problem which is NP-Complete. In this paper we express a theoretical framework for the NBV problem as an integer programming problem including a registration constraint. Experimental view planning results using a modified greedy search algorithm are presented.

1 Introduction

Automated acquisition of 3D geometric object models with active range sensors remains an open problem. The acquisition process involves an iterative cycle of view planning, sensing, registration and integration. Conventional non-model-based view planning methods can be categorized by the domain of reasoning about viewpoints - that is, surface, volume or global attributes. The most common surface-based method exploits occlusion edges, for example [7], while solid geometry algorithms have been used [14] to model volumetric object knowledge. Model-based approaches to view planning have the useful attribute of separating scene exploration from precision measurement [10]. The first phase captures a sparsely-sampled, approximate geometric object model by fast preprogrammed scans. Using this polygonal mesh rough model as the new knowledge base, a subsequent phase undertakes view planning for fine-detail, precise object scanning. More in-depth literature reviews can be found at [15], [10].

This paper addresses *performance-oriented* reconstruction which has been defined [10] as model acquisition based on explicit quality requirements expressed in a *model specification*. In addition to all-aspect coverage, typical quality objectives include measurement precision and sampling density, which may be constant or variable by region.

The key model-based view planning data structure is a *measurability matrix*, a concept first introduced for the inspection application by Tarbox and Gottschlich [16]. By convention, rows correspond to surface points and columns to viewpoints. Each matrix element is a binary estimate of the ability of the corresponding viewpoint to measure a specific rough model surface point. To be measurable, the surface point must be visible from both the optical transmitter (laser) and optical receiver (detector), and estimated measurement precision and sampling density must be within specified limits.

A measurability matrix is a powerful but computationally expensive view planning tool - $\mathcal{O}(s^2v)$, where $s = |S|$ and $v = |V|$ are the sizes of the surface and viewpoint sets, respectively. Sampling schemes in surface and viewpoint space are therefore important. While the required rough model sampling density depends on object shape complexity and specified reconstruction fidelity, experiments have shown that a fairly coarse rough model suffices for view planning and the process is robust with respect to modest levels of acquisition noise [12]. Viewpoint space decimation is even more critical as its dimensionality is much higher. Viewpoints are treated as generalized viewpoints $(\mathbf{v}, \lambda_\mathbf{v})$, consisting of sensor pose $\mathbf{v}$ and a set of controllable sensor parameters $\lambda_\mathbf{v}$. Experiments have shown that generation of approximately one optimized viewpoint per rough model surface point is usually sufficient.

As an additional measure to reduce computational complexity, the rough model may segmented into patches based on the view planning challenge presented by their shape. For example, cavities are particularly difficult to image due to shadow effects. In this case, a measurability matrix is computed for each segmented region. The cardinality of s and v are typically in the range [200,400] per patch. This compares with the size of a representative target fine model of about 10^5 points while brute force discretization of a one cubic meter imaging volume would require about 10^{11} viewpoints, even with pruning infeasible orientations.

Within this framework, view planning proceeds as follows - rough model creation by rapid pre-programmed scans, rough model segmentation (optional), viewpoint generation, measurability matrix computation, followed by solution of the set covering problem (SCP).

Industrial imaging environments often face an additional challenge with a positioning system whose accuracy falls below that of the sensor and the desired model precision. Such cases necessitate image-based registration (such as the standard Iterative Closest Point (ICP) algorithm [3]) to bring images into a common reference frame with a precision comparable to surface measurements. In the current work, we add an image-based registration constraint to the view planning problem (VPP) and present experimental view planning results using a modified greedy search (GS) algorithm with a registration constraint.

2 Image-Based Registration Constraint

Image-based registration requires sufficient overlap between images[1]. A degree of image overlap is also necessary for image integration. As a first approximation, this initial algorithm specifies a point overlap constraint which is necessary but not sufficient for image-based registration. In general, we need to add a geometric complexity requirement to the overlap region to fully constrain registration in all directions and rotations. It will be apparent from the simpler point overlap constraint how, in principal, we can formulate a more stringent constraint for overlap with geometric complexity. Development of a geometric complexity constraint is being pursued.

Image overlap can be determined from the degree of viewpoint correlation. For view planning purposes, we define the cross-correlation σ_{kj} of two viewpoints v_k and v_j as the dot product of the respective column vectors $\mathbf{M}_{S,k}$ and $\mathbf{M}_{S,j}$ of the measurability matrix, normalized[2] by the maximum surface coverage of any viewpoint in the candidate viewpoint set, i.e. $m_S = max|\mathbf{M}_{S,k}| \; \forall k \in V$.

$$\sigma_{kj} = \frac{\mathbf{M}_{S,k} \cdot \mathbf{M}_{S,j}}{m_S} \tag{1}$$

To register image (viewpoint) v_k with image (viewpoint) v_j with sufficient overlap, we require that their cross-correlation exceed a registration threshold, typically around 20%.

$$\sigma_{kj} \geq t_r \tag{2}$$

Let the binary variable $X_{kj} = 1$ if $\sigma_{kj} \geq t_r$ and $X_{kj} = 0$ otherwise. We can then compute the symmetric v-by-v *cross-correlation matrix* $\Sigma = [X_{kj}]$. Normally, $X_{kk} = 1$. In the rare case where $X_{kk} = 0$, meaning the image is so sparse it could not even register with itself, we drop the associated viewpoint from the candidate viewpoint list and reformulate the set covering problem accordingly.

We can now observe that Σ specifies viewpoint adjacency in registration terms. We therefore define a *viewpoint registration-adjacency matrix* $A = [a_{kj}]$ such that $a_{kj} = X_{kj}$, $k \neq j$, and $a_{kk} = 0$. The registration-adjacency matrix A has an associated *viewpoint registration graph* G_r encoding viewpoint connectivity in terms of inter-image registration potential. Consequently, we can express the view planning image-based registration requirement by stating that

The viewpoint registration graph must be at least simply connected.

Note that the viewpoint registration graph for each patch is a sub-graph of the global registration graph for the entire object. We can ensure global connectivity at the object level by an initial segmentation with suitable overlap across segmentation boundaries.

3 Set Covering Problem

3.1 View Planning as an Integer Programming Problem

We have previously developed [10] a set theory based formulation of the view planning problem in terms of a measurability mapping $\mathbf{v}_j \xrightarrow{\mathcal{M}} S_j$ between viewpoint space V and object surface space S. The set S_j of surface elements measurable by a single viewpoint $\mathbf{v}_j$ is defined by the corresponding column vector $\mathbf{M}_{S,j}$ of the measurability matrix. Similarly, the region V_i of viewpoint space from which a given surface element $\mathbf{s}_i$ is measurable is defined by the corresponding row vector $\mathbf{M}_{i,V}$ of the measurability matrix. Subsequently, the VPP was shown to be isomorphic to the SCP which is known to be NP-complete [5].

Recognizing the view planning problem as an instance of the set covering problem admits its expression as a classical 1/0 integer programming problem (IP), a sub-class of linear programming problems (LP). The VPP can be expressed as the problem of covering the rows of a binary s-by-v measurability matrix $\mathbf{M} = [m_{ij}]$ by a minimal subset of the columns.

We define the following variables: a vector $\mathbf{X}$ of binary viewpoint variables x_j, where $x_j = 1$ if measurability matrix column j is in the solution and $x_j = 0$ if not; a viewpoint cost c_j(non-uniform for significant positioning system movement cost, otherwise 1); and a *cumulative registration-adjacency matrix* $C = [c_{kj}]$ defining the number of paths in the registration graph of all lengths from minimum to maximum connectivity between viewpoints. In principal, C can be computed directly from Σ as a preprocessing step prior to tackling the IP problem [11].

Then, the view planning problem can be expressed as the following integer programming problem [11].

$$\text{Minimize } Z = \sum_{j=1}^{v} c_j x_j \tag{3}$$

subject to

$$\sum_{j=1}^{v} m_{ij} x_j \geq 1 \; ; \; i = 1, \ldots, s \; ; \; i \in S \tag{4}$$

$$c_{kj} \geq x_k x_j \; ; \; k = 1, \cdots, (v-1) \; ; \; j = k+1, \cdots, v \; ; \; k, j \in V \tag{5}$$

$$x_j \in \{0, 1\} \; ; \; j = 1, \ldots, v \; ; \; j \in V \tag{6}$$

[1] Few view planning techniques in the literature incorporate a registration constraint. Pito [8] includes an explicit overlap requirement and mentions the need for shape complexity in the overlap area but does not implement it. Whaite and Ferrie [17] achieve image overlap by a conservative search strategy.

[2] There are several potential choices for a normalizing value. m_S has the advantage of guaranteeing σ_{kj} values in the range [0,1], is reciprocal and is independent of segmentation patch size, object size, rough model sampling density and sensor characteristics.

Equation 3 states the minimization objective function and provides the option of assigning non-uniform costs to sensor movement; equation 4 expresses the set-covering requirement that each surface point be measured by at least one viewpoint; equation 5 imposes an image-based registration requirement that the registration graph for the segment be connected; and finally, equation 6 applies a binary constraint on viewpoint selection. The range of indices in equation 5 indicates we are interested only in the upper right triangle of the cumulative adjacency matrix.

3.2 Set Covering Algorithms

Expressing the view planning task as an IP provides a compact mathematical formulation of the problem, opening the application to the rich research base in discrete combinatorial optimization. Unfortunately, in general an integer programming problem is considerably more difficult to solve than the equivalent LP problem. IP solution time can be highly unpredictable, depending on problem formulation, data characteristics and problem size (number of variables and number of constraints). Optimal solution methods such as branch-and-bound and cutting-plane techniques typically use an intelligent tree search of feasible solutions and are found in a variety of commercial LP/IP solvers. While guaranteeing optimal results, such exact methods can be computationally prohibitive even for modestly sized IPs. For most medium-to-large IPs, this leaves a choice of approximate and heuristic algorithms [9], including greedy search (GS) [4], simulated annealing (SN) [13], genetic algorithm (GA) [2], Lagrangian relaxation [1] and neural network [6] methods. Most published performance results [6], [1] deal with random, low density data sets. The VPP falls into the category of a medium-to-large IP with non-random data and moderate density. A representative size for a measurability matrix generated by our algorithm will be approximately 400 variables by an equal number of constraints, or about $2\text{x}10^5$ elements.

3.3 Footprint Ratio

The problem of covering a surface patch can be characterized by its shape or size relative to sensor coverage. Convenient shape measures include depth-to-width ratio D/W for convex and concave patches. Relative size can be characterized by the following measures: the *patch footprint* F_p equal to the patch area and the *sensor footprint* F_s equal to the frustum cross-sectional area at the sensor's optimal scanning range R_o. A surface patch's *footprint ratio* $r_f = F_p/F_s$ provides a rough indication of the match between patch size, sensor capability and number of views required. However, recall that measurability images vary in size and shape and almost always cover less than 100 percent of the surface falling within the sensor frustum. Consequently, set covering operations involve set templates of variable size and shape. The absolute lower bound on the number of views required to cover a patch is $\lceil r_f \rceil$ - attainable only under the most optimistic scenario of a beneficial match between the shape of the patch and measurability images.

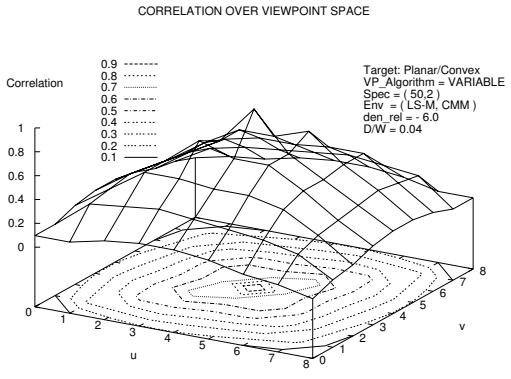

Figure 1: Viewpoint Correlation - Planar/Convex

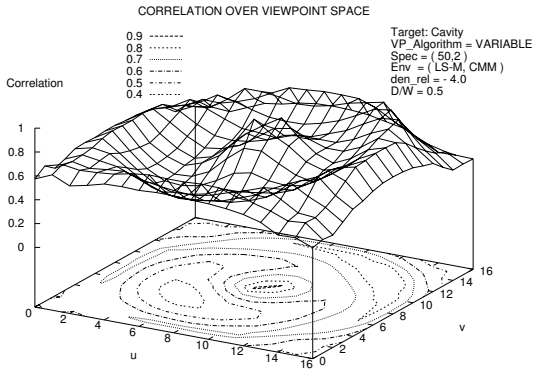

Figure 2: Viewpoint Correlation - Cavity

3.4 The VPP Solution Landscape

To test our algorithm, we generated two synthetic surface patches, the first larger than the sensor footprint and nearly planar, and the second smaller than the sensor footprint with a cavity shape. Figures 1 and 2 show viewpoint correlation relative to the mesh's center vertex as a function of translation in viewpoint space for the test patches. The axis of symmetry corresponds to the sensor optical baseline. The data indicates that neighbouring viewpoints are highly correlated, as expected, and that correlation falls off with displacement and is modified by surface shape. The footprint ratios are 2.55 and 0.55 respectively, while the measurability matrix densities are 0.238 and 0.637.

Thus, in contrast to many SCP applications reported in

the literature [6], variables in the VPP SCP application exhibit a high degree of correlation within neighbourhoods. Additionally, we note that constraint matrix densities are medium to high relative to other SCP applications. Finally, as in standard SCP applications, VPP solutions are generally not unique.

A VPP set covering algorithm must contend with competing forces acting on viewpoints in a candidate NBV set - a repelling force minimizing viewpoint correlation to gain coverage and an attracting force to achieve a minimum correlation level to maintain compliance with the registration constraint. A physics-based VPP set covering algorithm may be possible based on this paradigm.

4 Greedy Search Set Covering

4.1 Experimental Process

The experimental process followed in this work is shown in Figure 3. A high density mesh such as the example at Figure 4 serves as a surrogate fine model. The fine model is decimated to create a rough model at a desired lower sampling density, after which surface noise may be added. An example coarsely-sampled, noisy rough model is shown at Figure 5. The rough model drives the view planning process, including viewpoint generation, measurability estimation and NBV set determination. Other inputs include imaging environment and model specifications. The former defines performance models for the sensor and positioning system. The latter specifies model quality objectives - presently in the form of the tuple (measurement precision, sampling density). The resulting view plans are executed against the parent fine model, closing the loop to provide verified measurability.

4.2 Greedy Search

In this section we show experimental results using the greedy search (GS) set covering algorithm. The standard GS algorithm begins by computing a figure of merit (FOM) for each non-selected viewpoint - that is, the ratio of currently uncovered surface points covered by a candidate viewpoint to the total currently uncovered. Then, greedy search simply selects the viewpoint with the highest FOM. The first experiment was conducted with a nearly planar patch ($D/W = 0.04$) whose area was moderately greater than the sensor footprint ($r_f = 2.55$). The absolute lower bound on the number of views required to cover this patch is $\lceil r_f \rceil = 3$. Visual inspection shows the real lower bound to be 4, given the actual shape of the patch and sensor footprint. The experiment was conducted at a low rough model relative sampling density $\rho_{rel} = -6.0$, a model specification of (50 μm, 2 s/mm^2) for a range camera whose best-case performance was approximately (10 μm, 10 s/mm^2). Relative sampling density is defined as $\log_2$ of the ratio between the sampling density of the rough and fine models. This case illustrates a set covering problem driven more by relative size than shape.

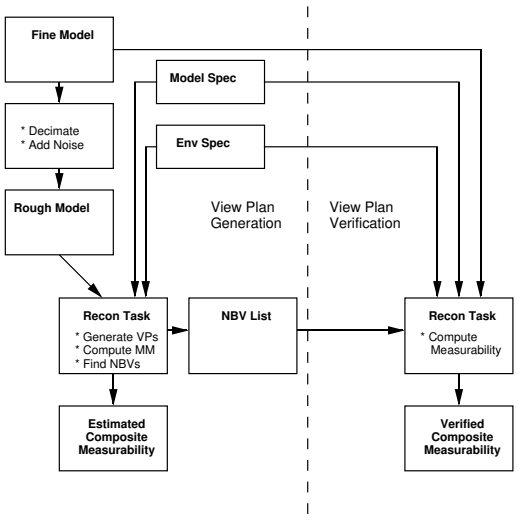

Figure 3: Experimental Process - Measurability Verification

Figure 4: Cavity Fine Model

Figure 5: Noisy Cavity Rough Model

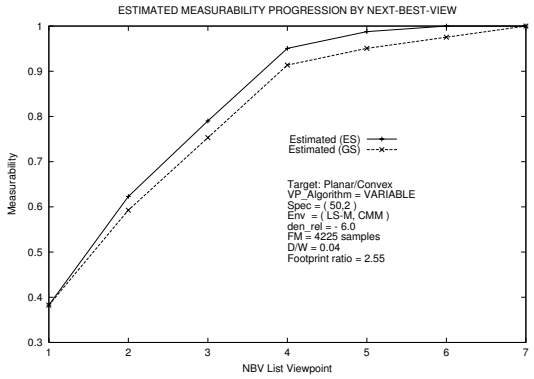

Figure 6: Estimated Measurability Progression

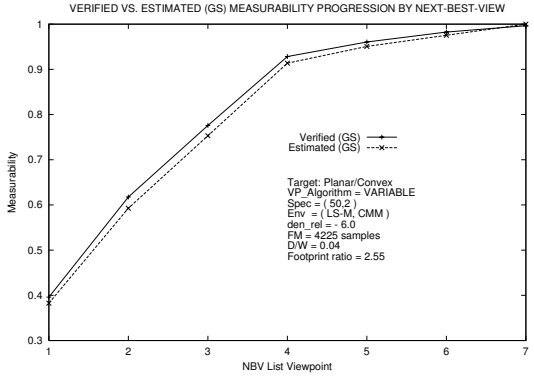

Figure 7: Verified Versus Estimated Measurability Progression

Figure 6 compares the progression of estimated measurability by the GS algorithm with the optimal solution obtained by exhaustive search (ES). The optimal curve represents the best achievable for any given size i of next-best-view set N_i. We note that greedy search results are compare favourably to the optimal (seven views required versus six), while the computational complexities are $\mathcal{O}(v^2)$ and exponential, respectively.

Figure 7 presents closed loop experimental results by verifying the computed NBV set against the fine model. Estimated measurability is very close to the verified performance, despite the low relative sampling density.

The NBV sequence generated by the GS algorithm is shown in Figure 8 on a u-v plot of the optimal scanning surface in viewpoint space. The u-v plot shows the relative position component of views. The surface patch maps to the range 0-120 over u and v. The GS set covering can be compared to the optimal set covering shown at Figure 9.

The matrix of raw cross-correlation valves for the GS next-best-view set at Figures 6, 7 and 8 is as follows.

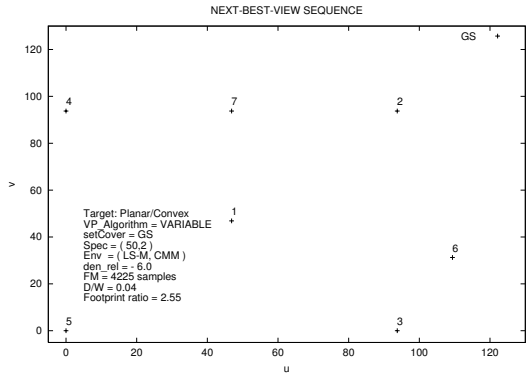

Figure 8: Next-Best-View Sequence (GS)

$$\begin{bmatrix} - & 0.326 & 0.097 & 0.097 & 0.326 & 0.226 & 0.387 \\ 0.326 & - & 0 & 0 & 0 & 0.194 & 0.355 \\ 0.097 & 0 & - & 0 & 0 & 0.452 & 0 \\ 0.097 & 0 & 0 & - & 0 & 0 & 0.326 \\ 0.326 & 0 & 0 & 0 & - & 0 & 0 \\ 0.226 & 0.194 & 0.452 & 0 & 0 & - & 0.065 \\ 0.387 & 0.355 & 0 & 0.326 & 0 & 0.065 & - \end{bmatrix}$$

From it we can deduce the connectivity of the registration graph G_r if various levels of t_r were applied post-facto. For example, for $t_r = 0.2$, the cross correlation matrix Σ is as follows. The graph is connected - in this case by statistical accident rather than by design.

$$\begin{bmatrix} - & 1 & 0 & 0 & 1 & 1 & 1 \\ 1 & - & 0 & 0 & 0 & 0 & 1 \\ 0 & 0 & - & 0 & 0 & 1 & 0 \\ 0 & 0 & 0 & - & 0 & 0 & 1 \\ 1 & 0 & 0 & 0 & - & 0 & 0 \\ 1 & 0 & 1 & 0 & 0 & - & 0 \\ 1 & 1 & 0 & 1 & 0 & 0 & - \end{bmatrix}$$

4.3 Constrained Greedy Search

We next add an image-based registration constraint to the standard GS algorithm. The NBV is now defined as the view with the maximum FOM that also maintains connectivity of the registration graph. This is achieved by requiring the NBV to meet the correlation threshold (register) with at least one member of the current NBV set.

Figure 10 shows NBV list size variation with the registration constraint. The data confirms that the number of views necessary to cover the surface patch increases with constraint severity. While list size plateaus over some ranges of the constraint, the composition of the NBV set and the structure of the registration graph are evolving with the changing overlap requirement. The algorithm begins to fail beyond a certain point as the problem becomes

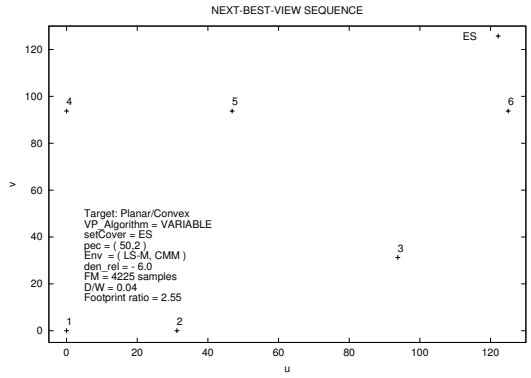

Figure 9: Next-Best-View Sequence (ES)

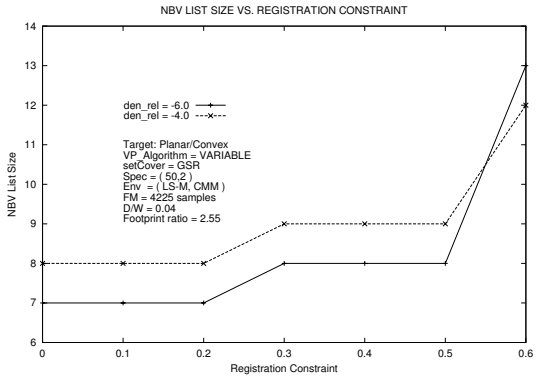

Figure 10: NBV List Size Versus Registration Constraint

over-constrained for the level of viewpoint space discretization. While this example of a moderately large and nearly planar patch illustrates the overlap-based approximation to the registration constraint, it is recognized that the viewpoint (image) sequence is not fully constrained for registration purposes in the absence of greater object shape complexity.

Figure 12 presents NBV positions in viewpoint space and their sequence, overlaid with the associated registration graph for values of t_r in the range [0.1, 0.6]. As the registration constraint is slowly tightened, we can observe subtle shifts in set covering and registration linkages. As specified, G_r maintains at least simple connectivity.

The matrix of raw cross-correlation values and corresponding cross-correlation matrix Σ for the constrained set covering problem at Figure 12(b) for $t_r = 0.2$ are as follows, which can be compared to that obtained in the unconstrained case.

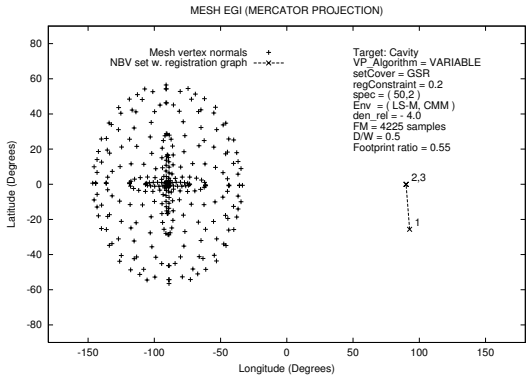

Figure 11: Mesh and NBV List EGI - Cavity

$$\begin{bmatrix} - & 0.326 & 0.258 & 0.258 & 0.326 & 0.226 & 0.387 \\ 0.326 & - & 0.129 & 0.129 & 0 & 0.194 & 0.355 \\ 0.258 & 0.129 & - & 0 & 0 & 0.581 & 0 \\ 0.258 & 0.129 & 0 & - & 0 & 0 & 0.516 \\ 0.326 & 0 & 0 & 0 & - & 0 & 0 \\ 0.226 & 0.194 & 0.581 & 0 & 0 & - & 0.065 \\ 0.387 & 0.355 & 0 & 0.516 & 0 & 0.065 & - \end{bmatrix}$$

$$\begin{bmatrix} - & 1 & 1 & 1 & 1 & 1 & 1 \\ 1 & - & 0 & 0 & 0 & 0 & 1 \\ 1 & 0 & - & 0 & 0 & 1 & 0 \\ 1 & 0 & 0 & - & 0 & 0 & 1 \\ 1 & 0 & 0 & 0 & - & 0 & 0 \\ 1 & 0 & 1 & 0 & 0 & - & 0 \\ 1 & 1 & 0 & 1 & 0 & 0 & - \end{bmatrix}$$

To illustrate a set covering problem driven more by shape than relative size, Figure 11 presents the view plan generated for a deep cavity surface patch with $D/W = 0.5$, $r_f = 0.55$ and measurability matrix density = 0.637. The data is presented in extended Gaussian image (EGI) format to highlight the orientation complexity of the patch. Two items are shown: the cavity mesh as represented by the angular distribution of surface normals and the axis component of each viewpoint in the NBV set overlaid with the registration graph. As expected, viewpoints are located on the opposite side of the Gaussian sphere from the mesh. To relate viewpoints to mesh orientations, their axis vector must be negated. Thus, viewpoints 2 and 3 (with the same axis but different rotation about that axis) are aligned with the cavity axis of symmetry while viewpoint 1 peers over the rim of the cavity into its depths. The registration graph is fully connected for $t_r = 0.2$ and the GS set covering is optimal.

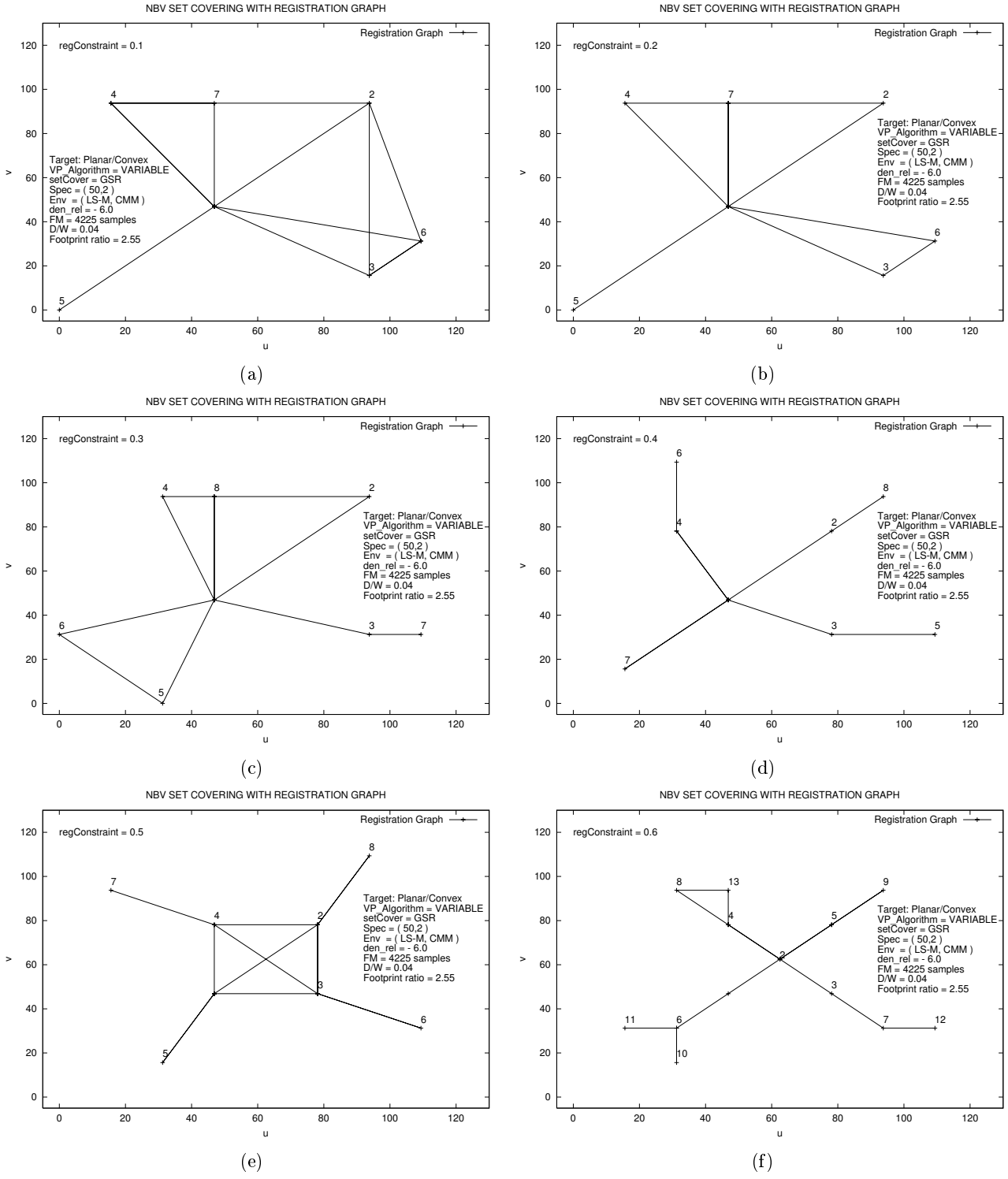

Figure 12: NBV Set Covering with Registration Graph

5 Summary and Conclusions

Experiments reported here have revealed both strengths and weaknesses of set covering by greedy search. Two problems in particular are noticeable. Firstly, close examination of Figure 7 reveals a small residual unmeasured region upon executing the complete NBV list. This artifact results from minor errors in surface normal estimation which translate into errors in viewpoint orientation and hence sensor footprint coverage. The problem manifests itself in small uncovered filets between verified measurability images. This can be corrected by slightly downsizing the sensor frustum volume used for measurability analysis. Secondly, in the nearly planar patch example, we note a discrepancy between the minimum number of views determined by visual inspection (4) and the optimal result (6) achieved by exhaustive search of candidate viewpoints. This is because the candidate viewpoint set does not optimally span viewpoint space. While these results are still quite good for the current very low level of viewpoint space sampling (one viewpoint per rough model vertex), there is room for further optimization. In particular, useful trade-offs can be made between discretization levels in orientation and position components of viewpoint space. These observations again illustrate that generation of a small set of high quality candidate viewpoints is the crux to efficiently solving the VPP. Viewpoint generation will be addressed in a separate paper.

The classic weakness of the greedy search algorithm, its irrevocable selection strategy [16], has minimal impact on most industrial and cultural object reconstruction applications. Typically, the object size is comparable to or smaller than the sensor frustum ($r_f < 1$) and shape presents the dominant view planning challenge. Cases of large r_f are the exception rather than the rule. Consequently, measurability matrix density is typically medium-to-high and solution set size is low relative to most set covering applications. In reconstruction, minor inefficiency resulting from a marginally longer NBV list is offset by fast and robust GS set covering computation plus added coverage insurance from redundancy. In contrast, inspection applications are generally prepared to trade longer off-line view plan computation for improved on-line view plan efficiency. In either case, we have presented a theoretical basis for computing optimal view plans by means of slightly more dense sampling of viewpoint space and more computationally intensive exact or heuristic set covering algorithms.

For object reconstruction, we find that greedy search gives good set covering results and believe that computational resources are best allocated to quality viewpoint generation. Phrased differently, we believe the most difficult challenge of the VPP is framing the problem, not solving it - that is, determining an appropriate set of viewpoint variables and surface constraints and computing the associated measurability matrices.

In conclusion, we have expressed a theoretical framework for the view planning problem as an integer programming problem including a registration constraint. The formulation is amenable to a variety of exact or approximate solution methods, depending on application requirements. We have also shown that good view planning results can be achieved by means of a simple and robust greedy search set covering algorithm modified to include a registration constraint. The constraint is being modified to include a geometric complexity requirement in the overlap region.

References

[1] J. Beasley. A lagrangian heuristic for set covering problems. *Naval Research Logistics*, 37:151–164, 1990.

[2] J. Beasley and P. Chu. A genetic algorithm for the set covering problem. *European Journal of Operational Research*, 94:392–404, 1995.

[3] P. J. Besl and H. D. McKay. A method for registration of 3d shapes. *IEEE Trans. PAMI*, 14(2):239–256, February 1992.

[4] M. Fisher and L. Wolsey. On the greedy heuristic for covering and packing problems. *SIAM Journal of Algebraic and Discrete Methods*, 3(4):584–591, Dec 1982.

[5] M. Garey and D. Johnson. *Computers and Intractability: A Guide to the Theory of NP-Completeness.* W.H. Freeman, 1979.

[6] T. Grossman and A. Wool. Computational experience with approximation algorithms for the set covering problem. *European Journal of Operational Research*, 101:81–92, 1997.

[7] J. Maver and R. Bajcsy. Occlusions as a guide for planning the next view. *IEEE Trans. PAMI*, 17(5):417–433, May 1993.

[8] R. Pito. A sensor based solution to the next-best-view problem. In *IEEE Int. Conf. on Robotics and Automation*, pages 941–945, August 1996.

[9] C. R. Reeves. *Modern Heuristic Techniques for Combinatorial Problems.* Blackwell Scientific Publications, Oxford, 1993.

[10] W. Scott, G. Roth, and J.-F. Rivest. Performance-oriented view planning for automatic model acquisition. In *31st Int. Symposium on Robotics, Montreal*, pages 314–319, May 2000.

[11] W. Scott, G. Roth, and J.-F. Rivest. View planning as a set covering problem. *Submitted to IEEE Trans. Robotics and Automation*, 2001.

[12] W. Scott, G. Roth, and J.-F. Rivest. View planning for multi-stage object reconstruction. In *Submitted to Vision Interface 01 Conf., Ottawa*, 2001.

[13] S. Sen. Minimal cost set covering using probabilistic methods. In *ACM Symp. Applied Computing, Indianapolis*, pages 157–164, 1993.

[14] I. Stamos and P. Allen. Interactive sensor planning. In *Proc. IEEE Conf. Vis. Pat. Rec., Santa Barbara, CA*, pages 489–494, June 23-25 1998.

[15] K. Tarabanis, P. K. Allen, and R. Y. Tsai. A survey of sensor planning in computer vision. *IEEE Trans. Robotics and Automation*, 11(1):86–104, February 1995.

[16] G. Tarbox and S. Gottschlich. Planning for complete sensor coverage in inspection. *Computer Vision and Image Understanding*, 61(1):84–111, January 1995.

[17] P. Whaite and F. P. Ferrie. Autonomous exploration: Driven by uncertainty. *IEEE Trans. PAMI*, 19(3):193–205, March 1997.